

Magnetic Ground-State of Perovskite  $\text{PbVO}_3$  with Large Tetragonal DistortionKengo Oka,<sup>\*†</sup> Ikuya Yamada,<sup>‡§</sup> Masaki Azuma,<sup>\*†</sup> Soshi Takeshita,<sup>||</sup> Kohki H. Satoh,<sup>⊥</sup> Akihiro Koda,<sup>||</sup> Ryosuke Kadono,<sup>||</sup> Mikio Takano,<sup>†#</sup> and Yuichi Shimakawa<sup>†</sup>

Institute for Chemical Research, Kyoto University, Uji, Kyoto 611-0011, Japan, Institut de Minéralogie et de Physique des Milieux Condensés, Université Pierre et Marie Curie, Paris 75015, France, Institute of Materials Structure Science, High Energy Accelerator Research Organization, KEK, Tsukuba, Ibaraki 305-0801, Japan, and The Graduate University for Advanced Studies, Tsukuba, Ibaraki 305-0801, Japan

Received April 11, 2008

The magnetic properties of  $\text{PbVO}_3$ , a  $\text{PbTiO}_3$ -type perovskite with a large tetragonal distortion ( $c/a = 1.229$ ), were investigated. The temperature dependence of the measured magnetization of multidomain single-crystal samples showed a broad maximum centered around 180 K, indicating a two-dimensional antiferromagnetism.  $\mu\text{SR}$  measurement revealed the presence of a long-range order below 43 K. The two-dimensional magnetism is due to the ordering of  $d_{xy}$  orbitals, which is thought to also be related to the large tetragonal distortion of  $\text{PbVO}_3$ .

## 1. Introduction

$\text{PbTiO}_3$ -based ferroelectric and piezoelectric materials are widely used in memory devices, actuators, and transducers. Both  $\text{Pb}^{2+}$  and  $\text{Ti}^{4+}$  contribute to the large tetragonal distortion in  $\text{PbTiO}_3$ .<sup>1,2</sup> The stereochemical effect of the  $6s^2$  lone-pair electrons in the  $\text{Pb}^{2+}$  ion and the covalent  $\text{Pb}-\text{O}$  bonds tend to stabilize distorted acentric structures. The hybridization between Ti 3d and O 2p states is also thought to be essential for the ferroelectricity of this compound. The search for practically useful ferroelectric and piezoelectric perovskites had been limited to the systems with  $d^0$  ions such as  $\text{Ti}^{4+}$ ,  $\text{Nb}^{5+}$ , and  $\text{Ta}^{5+}$  in the B-sites. The large spontaneous polarization found in  $\text{BiFeO}_3$  thin films,<sup>3</sup> however, suggests that investigations of Bi and Pb perovskites with other transition elements might lead to new high-performance

ferroelectric and piezoelectric materials. This is because  $\text{Bi}^{3+}$  ion has the same electronic configuration and similar character with  $\text{Pb}^{2+}$ .  $\text{BiFeO}_3$  and  $\text{PbTiO}_3$  are the only Bi and Pb 3d transition metal perovskites that can be prepared at ambient pressure. We have investigated others stabilized at high pressures<sup>4–7</sup> and found that  $\text{PbVO}_3$ <sup>8,9</sup> and  $\text{BiCoO}_3$ <sup>10</sup> are isostructural with tetragonal  $\text{PbTiO}_3$ , as illustrated in the inset of Figure 3a, but have tetragonal distortions ( $c/a = 1.229$  for  $\text{PbVO}_3$  and 1.267 for  $\text{BiCoO}_3$ ) much larger than that of  $\text{PbTiO}_3$  ( $c/a = 1.062$ ). Other Bi-, Pb-containing perovskites

\* To whom correspondence should be addressed. E-mail: oka@msk.kuicr.kyoto-u.ac.jp (K.O.), masaki@scl.kyoto-u.ac.jp (M.A.). Phone: +81-774-38-3115(K.O.), +81-774-38-3113(M.A.). Fax: +81-774-38-3118 (K.O.), +81-774-38-3118 (M.A.).

† Kyoto University.

‡ Université Pierre et Marie Curie.

§ Current address: Graduate School of Science and Engineering, Ehime University, 2-5 Bunkyo-Cho, Matsuyama 790-8577, Japan.

|| High Energy Accelerator Research Organization.

⊥ The Graduate University for Advanced Studies.

# Current address: Institute for Integrated Cell-Material Sciences, Kyoto University; c/o Research Institute for Production Development, 15 Shimogamo Morimoto-cho, Sakyo-ku, Kyoto 606-0805, Japan.

(1) Cohen, R. E. *Nature* **1992**, *358*, 136.

(2) Kuroiwa, Y.; Aoyagi, S.; Sawada, A.; Harada, J.; Nishibori, E.; Takata, M.; Sakata, M. *Phys. Rev. Lett.* **2001**, *87*, 217601.

(3) Wang, J.; Neaton, J. B.; Zheng, H.; Nagarajan, V.; Ogale, S. B.; Liu, B.; Viehland, D.; Vaithyanathan, V.; Schlom, D. G.; Waghmare, U. V.; Spaldin, N. A.; Rabe, K. M.; Wuttig, M.; Ramesh, R. *Science* **2003**, *299*, 1719.

(4) Azuma, M.; Takata, K.; Saito, T.; Ishiwata, S.; Shimakawa, Y.; Takano, M. *J. Am. Chem. Soc.* **2005**, *127*, 8889.

(5) Sakai, M.; Masuno, A.; Kan, D.; Hashisaka, M.; Takata, K.; Azuma, M.; Takano, M.; Shimakawa, Y. *Appl. Phys. Lett.* **2007**, *90*, 072903.

(6) Ishiwata, S.; Azuma, M.; Takano, M.; Nishibori, E.; Takata, M.; Sakata, M.; Kato, K. *J. Mater. Chem.* **2002**, *12*, 3733.

(7) Azuma, M.; Carlsson, S.; Rodgers, J.; Tucker, M. G.; Tsujimoto, M.; Ishiwata, S.; Isoda, S.; Shimakawa, Y.; Takano, M.; Attfield, J. P. *J. Am. Chem. Soc.* **2007**, *129*, 14433.

(8) Belik, A. A.; Azuma, M.; Saito, T.; Shimakawa, Y.; Takano, M. *Chem. Mater.* **2005**, *17*, 269.

(9) Shpanchenko, R. V.; Chernaya, V. V.; Tsirlin, A. A.; Chizhov, P. S.; Sklovsky, D. E.; Antipov, E. V.; Khlybov, E. P.; Pomjakushin, V.; Balagurov, A. M.; Medvedeva, J. E.; Kaul, E. E.; Geibel, C. *Chem. Mater.* **2004**, *16*, 3267.

(10) Belik, A. A.; Iikubo, S.; Kodama, K.; Igawa, N.; Shamoto, S.; Niitaka, S.; Azuma, M.; Shimakawa, Y.; Takano, M.; Izumi, F.; Takayama-Muromachi, E. *Chem. Mater.* **2006**, *18*, 798.

did not crystallize with this structure.  $\text{PbCrO}_3$  is cubic.<sup>11</sup>  $6s^2$  lone pairs are arranged antiparallel in  $\text{BiCrO}_3$ ,<sup>12</sup>  $\text{BiMnO}_3$ ,<sup>13</sup> and  $\text{BiNiO}_3$ .<sup>6,7</sup>  $\text{BiFeO}_3$  is rhombohedral with electric polarization along the  $[111]$  direction.<sup>3</sup> Therefore, the large tetragonal distortions cannot be attributed only to the stereochemical effect of  $\text{Pb}^{2+}$  and  $\text{Bi}^{3+}$  ions. It is necessary to understand the origin of such large distortions for further material search.

Other interesting aspects of these compounds are their magnetic behaviors.  $\text{BiCoO}_3$  is an antiferromagnet with a Néel temperature ( $T_N$ ) of 420 K and with the  $C$ -type spin structure.<sup>10</sup> The magnetic susceptibility of polycrystalline samples of  $\text{PbVO}_3$  indicates that  $\text{PbVO}_3$  is a two-dimensional  $S = 1/2$  square lattice antiferromagnet like  $\text{Li}_2\text{VOSiO}_4$ .<sup>14</sup> The ratio of the next-nearest-neighbor interaction ( $J_2$ ) to the nearest neighbor one ( $J_1$ ) was estimated to be 0.38 by high temperature series expansions, indicating this system had a magnetic frustration. The intrinsic magnetic property, however, was not clear because the samples contained ferromagnetic impurities. Although  $C$ -type or  $G$ -type ordering was predicted by first-principle calculations,<sup>15,16</sup> a neutron powder diffraction study performed by Shpanchenko et al. at temperatures down to 1.5 K found no evidence of long-range magnetic ordering.<sup>9</sup>

In this paper, we report on the magnetic ground-state of  $\text{PbVO}_3$ . We show that the magnetization data for a multi-domain single-crystal sample without magnetic impurities showed the characteristic features for a two-dimensional antiferromagnet and a sharp rise indicating a magnetic transition at 50 K. We also show the results of muon spin rotation ( $\mu\text{SR}$ ) measurements confirming the long-range antiferromagnetic ordering below 43 K. We then discuss the origin of the large tetragonal distortion of  $\text{PbVO}_3$  and  $\text{BiCoO}_3$  in terms of its relation to the two-dimensional magnetism of  $\text{PbVO}_3$ .

## 2. Experimental Section

$\text{PbVO}_3$  was prepared under high-pressure (HP) and high-temperature (HT) conditions in a cubic anvil type HP apparatus. A polycrystalline sample for  $\mu\text{SR}$  measurement was prepared from a stoichiometric mixture of  $\text{PbO}$ ,  $\text{V}_2\text{O}_3$ , and  $\text{V}_2\text{O}_5$ . The mixture was sealed in a gold capsule and treated at 6 GPa and 1173 K for 30 min as described before.<sup>8</sup> Single crystals were grown from the same mixture with 10 wt % of distilled water sealed in a platinum capsule. A synchrotron X-ray powder diffraction study was performed under HP and HT conditions at the BL14B1 beamline of SPring-8 to determine the crystal growth condition. The white beam X-ray was incident to the sample in the HP cell, and the diffraction was detected by a solid-state detector fixed at  $2\theta = 4.5$  deg. The details

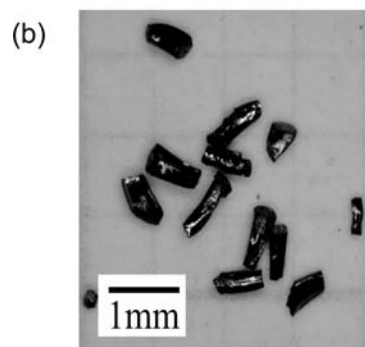
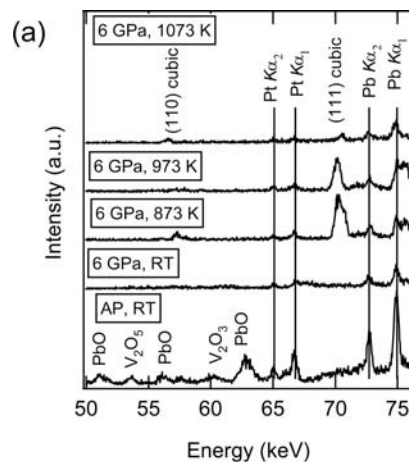


**Figure 1.** (a) Synchrotron X-ray powder diffraction patterns of  $\text{PbO} + \text{V}_2\text{O}_3 + \text{V}_2\text{O}_5$  mixed with 10 wt % water under various conditions. The four vertical lines in the figure stand for the characteristic X-rays of Pb ( $\text{K}\alpha_1$ ,  $\text{K}\alpha_2$ ) and Pt ( $\text{K}\alpha_1$ ,  $\text{K}\alpha_2$ ) generated from the sample and the capsule. (b) The photograph of obtained single-crystalline  $\text{PbVO}_3$ .

of the experiment are described elsewhere.<sup>17</sup> The magnetization was measured with a SQUID magnetometer (Quantum Design, MPMS XL) in an external field of 1000 Oe on about six pieces of crystals with the total mass of 2.3 mg. Because of the twinning of the crystals, the specimens were not aligned to any specific crystallographic axis.  $\mu\text{SR}$  measurements were conducted on the M-15 beamline of TRIUMF. The samples for those measurements were crushed into powders, molded into disk shapes, solidified with glue, and then mounted on a stage.

## 3. Results

**Single-Crystal Growth of  $\text{PbVO}_3$ .** Since there are quite a few reports on single-crystal growth of vanadium oxides by hydrothermal reaction,<sup>18</sup> we tried to grow  $\text{PbVO}_3$  crystals in the presence of water. The synchrotron X-ray powder diffraction patterns of  $4\text{PbO} + \text{V}_2\text{O}_3 + \text{V}_2\text{O}_5$  mixed with 10 wt % water under HP and HT conditions are shown in Figure 1a, where one sees that at 6 GPa and 873 K the mixture reacted to form a cubic perovskite of  $\text{PbVO}_3$ . At 1073 K the diffraction peak intensities were significantly reduced, indicating that the solid phase started to dissolve in the water. Single-crystal growth was conducted in an in-house HP apparatus. The same mixture was sealed in a

(11) Arevalo-Lopez, A. M.; Alario-Franco, M. A. *J. Solid State Chem.* **2007**, *180*, 3271.

(12) Niitaka, S.; Azuma, M.; Takano, M.; Nishibori, E.; Takata, M.; Sakata, M. *Solid State Ionics* **2004**, *172*, 557.

(13) Belik, A. A.; Iikubo, S.; Yokosawa, T.; Kodama, K.; Igawa, N.; Shamoto, S.; Azuma, M.; Takano, M.; Kimoto, K.; Matsui, Y.; Takayama-Muromachi, E. *J. Am. Chem. Soc.* **2007**, *129*, 971.

(14) Tsirlin, A. A.; Belik, A. A.; Shpanchenko, R. V.; Antipov, E. V.; Tkayama-Muromachi, E.; Rosner, H. *Phys. Rev. B* **2008**, *77*, 092402.

(15) Uratani, Y.; Shishidou, T.; Ishii, F.; Oguchi, T. *Jpn. J. Appl. Phys.* **2005**, *44*, 7130.

(16) Singh, D. *J. Phys. Rev. B* **2006**, *73*, 094102.

(17) Saito, T.; Terashima, T.; Azuma, M.; Takano, M.; Goto, T.; Ohta, H.; Utsumi, W.; Bordet, P.; Johnston, D. C. *J. Solid State Chem.* **2000**, *153*, 124.

(18) Chirayil, T.; Zavalij, P. Y.; Whittingham, M. S. *Chem. Mater.* **1998**, *10*, 2629.

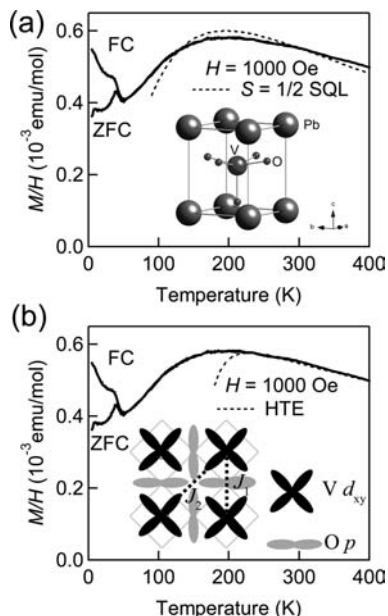


**Figure 2.** Temperature dependence of magnetization divided by the field ( $M/H$ ) of a single-crystal  $\text{PbVO}_3$  sample measured on heating after zero-field cooling and on cooling in an applied field of 1000 Oe. The dashed line in panel a shows the result of fitting to the  $S = 1/2$  square lattice model ( $S = 1/2$  SQL), and the dashed line in panel b is the result calculated by high-temperature series expansions (HTE) of the  $J_1$ - $J_2$  model with the parameters as given in the text. The insets in panels a and b show the crystal structure of  $\text{PbVO}_3$  and the magnetic exchange pathways, respectively.

platinum capsule and then compressed to 6 GPa. The temperature was raised to 1223 K, kept for 30 min, and then slowly cooled to 973 K for 12 h before releasing the pressure. Figure 1b shows the crystals that were obtained. Their phase purity was verified by X-ray diffraction measurement on crushed powders. The oscillation photograph (not shown) revealed that these crystals have multiple domains probably due to the change from cubic to tetragonal symmetry during the pressure release.<sup>8</sup>

**Magnetization Measurement.** The temperature dependence of the magnetization of single-crystal  $\text{PbVO}_3$  divided by the field ( $M/H$ ) is shown in Figure 2. The broad maximum centered around 180 K is characteristic of a low-dimensional antiferromagnetic system. The first-principle calculation by Uratani et al.<sup>15</sup> indicated that the  $d_{xy}$  orbital is the only one of the three  $t_{2g}$  orbitals that is occupied by one electron, so  $\text{PbVO}_3$  is expected to be two-dimensional in magnetism. The data between 100 and 400 K were therefore fitted to the following  $S = 1/2$  square lattice model<sup>19</sup> with a temperature-independent term,

$$\chi(T) = \frac{Ng^2\mu_B^2}{4k_B T} \left[ 1 + \left( \frac{J}{k_B T} \right) + \frac{1}{2} \left( \frac{J}{k_B T} \right)^2 + \frac{1}{6} \left( \frac{J}{k_B T} \right)^3 + \frac{1}{64} \left( \frac{J}{k_B T} \right)^4 \right]^{-1} + \chi_0 \quad (1)$$

where  $N$  is the Avogadro constant,  $g$  is the gyromagnetic ratio (fixed to 2),  $J$  is the nearest-neighbor exchange, and  $k_B$  is the Boltzmann constant. The fitting gave  $J = 205(2)$  K

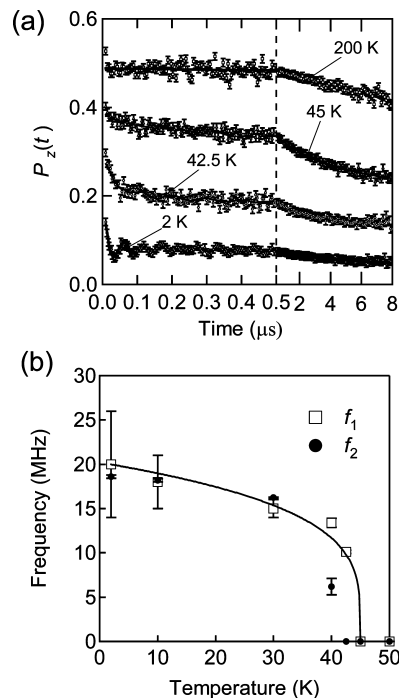


**Figure 3.** (a) ZF- $\mu$ SR time spectra of polycrystalline  $\text{PbVO}_3$  measured at various temperatures. The left and the right columns correspond to the time ranges of 0–0.5  $\mu$ s and 0.5–8  $\mu$ s, respectively. The open circles and the solid curves represent the observed and the fitted data, respectively. The spectra of 42.5 K, 45 K, and 200 K were respectively offset by 0.1, 0.2, and 0.3. (b) Temperature dependence of the muon spin precession frequencies  $f_1$  and  $f_2$  in  $\text{PbVO}_3$ . The curve is the result of fitting the  $f_1$  data to  $A(T_N - T)^\nu$ , with the parameters given in the text.

and  $\chi_0 = -7.9(6) \times 10^{-5}$  emu/mol, but the quality of the fit was rather poor. Because the nearest-neighbor interaction ( $J_1$ ) is mediated by the  $t_{2g}$ -O  $2p$ - $t_{2g}$  bonds that have  $\pi$  overlaps as illustrated in the inset of Figure 2a, its magnitude is relatively small. As discussed by Tsirlin et al.,<sup>14</sup> in such a case the contribution of the second nearest-neighbor interaction ( $J_2$ ) is not negligible. Because there is no analytical formula for the  $J_1$ - $J_2$  model in the entire temperature range, we estimated the  $J_2/J_1$  ratio that governs the magnetic ground-state by carrying out high-temperature series expansions with the  $J_1$ - $J_2$  Heisenberg model by Rosner et al.<sup>20</sup> for the data between 200 and 400 K. As shown in Figure 2b, the best fit was obtained with  $J_1 = 190$  K,  $J_2/J_1 = 0.32$ , and  $\chi_0 = 1.4 \times 10^{-4}$  emu/mol. The magnitude of  $J_1$  was almost identical to that estimated for the simple square lattice model, confirming the validity of this analysis. The  $J_2/J_1$  ratio, however, was considerably smaller than the 0.38 previously estimated for a polycrystalline sample,<sup>14</sup> probably because the polycrystalline sample contained magnetic impurities such as  $\text{VO}_2$  and  $\text{PbV}_6\text{O}_{11}$ .

With further decreasing temperature, a sharp rise was observed at 50 K followed by a kink at 40 K. Such anomalies were also observed in the data for the polycrystalline sample,<sup>14</sup> but they are more pronounced in our single-crystal data. Below 40 K the zero-field cooled (ZFC) data deviate from the field-cooled (FC) data, indicating the presence of a

(19) Johnston, D. C. In *Handbook of Magnetic Materials*; Buschow, K. H. J., ed.; North-Holland: Amsterdam, 1997; Vol. 10.

(20) Rosner, H.; Singh, R. R. P.; Zheng, W. H.; Oitmaa, J.; Pickett, W. E. *Phys. Rev. B* **2003**, *67*, 014416.



magnetic transition. The question is whether it is long-range ordering or a spin-glass-like freezing.

**$\mu$ SR Measurement.** The magnetic ground-state of  $\text{PbVO}_3$  was further investigated by making  $\mu$ SR measurements because this technique is the one most sensitive to the magnetic ordering. Figure 3a shows the zero-field  $\mu$ SR (ZF- $\mu$ SR) spectra measured at various temperatures. Clear oscillation patterns indicating long-range antiferromagnetic ordering were observed below 42.5 K, consistent with the magnetization data. The data at 200 K showed a slow relaxation and were well fitted with the Gaussian Kubo–Toyabe function  $G_{\text{KT}}$ . This slow relaxation is due to  $^{51}\text{V}$  and  $^{207}\text{Pb}$  nuclear magnetic moments. For the analysis of the data measured at lower temperatures, the estimated initial amplitude of  $A_{200\text{K}} = 0.1875(8)$  was used as the total amplitude. The data below 50 K were analyzed using the following formula assuming two oscillating components and one nonoscillating component

$$P(t) = A_1 \exp(-\lambda_1 t) \cos(2\pi f_1 t + \phi) + A_2 \exp(-\lambda_2 t) \cos(2\pi f_2 t + \phi) + A_3 \exp[-(\lambda_3 t)^\beta] \quad (2)$$

where  $A_1$ ,  $A_2$ , and  $A_3$  are the asymmetries,  $\lambda_1$ ,  $\lambda_2$ , and  $\lambda_3$  are the relaxation rates,  $f_1$  and  $f_2$  are the muon spin precession frequencies,  $\phi$  is the phaselag, and  $\beta$  is the power of the exponent. The first two terms correspond to the oscillating components and the third one corresponds to the nonoscillating component. The oscillating components are due to muons stopping at a site where the local field is parallel to the initial spin polarization, and the nonoscillating components are due to muons stopping at a site where the local field is perpendicular to the initial spin polarization. At 2 K  $A_1 = 0.0873(9)$  and  $A_2 = 0.0159(13)$ . The proportion of  $(A_1 + A_2)/A_{\text{total}}$  ( $A_{\text{total}} = A_1 + A_2 + A_3 = A_{200\text{K}}$ ) is approximately 2/3 that expected for a randomly oriented polycrystalline sample with a long-range magnetic ordering, confirming the long-range ordering in the whole sample. The two oscillation frequencies were determined to be  $f_1 = 20(6)$  MHz and  $f_2 = 18.57(17)$  MHz. It should be noted that these values are close to the 16 MHz observed for an  $S = 1/2$  two-dimensional antiferromagnet  $\text{Ca}_{0.86}\text{Sr}_{0.14}\text{CuO}_2$  with “infinite layer” structure<sup>21</sup> supporting the two-dimensional nature of the magnetism in this system. The relaxation of the first oscillating component is quite fast,  $\lambda_1 = 83(9) \mu\text{s}^{-1}$ , while that of the second oscillating component is slow,  $\lambda_2 = 4.6(7) \mu\text{s}^{-1}$ . For the nonoscillating component,  $\lambda_3 = 0.044(5) \mu\text{s}^{-1}$  and  $\beta = 0.57(4)$  were obtained. It is known that the positive muons stop around  $\text{O}^{2-}$  with a distance of  $\sim 1 \text{ \AA}$ .<sup>22</sup> Considering the two-dimensionality in magnetism, we tentatively assign the component with fast relaxation to the muons stopped at the apical oxygen site under an inhomogeneous field along the  $c$  axis and the component with slow relaxation to the muons stopped at the in-plane oxygen site.

The 10, 30, 40, 42.5, 45, and 50 K data were also analyzed to clarify the temperature evolutions of the oscillation

frequencies. Figure 3b shows  $f_1$  and  $f_2$  as functions of temperature. Both  $f_1$  and  $f_2$  showed almost the same behaviors, vanishing at around 45 K and thus clearly showing the development of long-range magnetic ordering. The curve in Figure 3b shows that the temperature dependence of  $f_1$  could be fitted using a power-law function  $A(T_N - T)^\gamma$  with  $T_N = 43(2)$  K and  $\gamma = 0.17(6)$ .

#### 4. Discussion

The results of our magnetic measurements were consistent with the first-principles calculation which predicted that  $\text{PbVO}_3$  is a two-dimensional antiferromagnet owing to the ordering of the  $d_{xy}$  orbital.<sup>15</sup> Although the system was frustrated (with  $J_2/J_1 = 0.32$ ) because the diagonal next-nearest-neighbor interaction was not negligible, it exhibited an antiferromagnetic long-range ordering at 50 K (inferred from the results of magnetization measurements)  $\sim 43$  K (inferred from the results of  $\mu$ SR measurements). Theoretical calculations have indicated that in the  $J_1$ – $J_2$  system the boundary between long-range ordering and the spin glass state lies at  $J_2/J_1 = 0.38$ ,<sup>23</sup> 0.34,<sup>24</sup> and 0.24.<sup>25</sup> Our estimation of  $J_2/J_1$  ratio is 0.32, so the observation of the long-range ordering suggests that the former two theoretical results are realistic. We suspect that although the magnetic ground-state of this compound is an antiferromagnetic long-range ordering, the magnetic Bragg peaks are not easily observed by neutron diffraction because of the small spin of  $S = 1/2$ , shrinkage of the ordered moment owing to two-dimensionality.<sup>26,27</sup>

Next, we would like to discuss the origin of the large tetragonal distortion of  $\text{PbVO}_3$ . The pyramidal coordination of  $\text{V}^{4+}$  is found in other  $\text{V}^{4+}$  oxides such as  $(\text{VO})_2\text{P}_2\text{O}_7$ ,<sup>28,29</sup> and  $\text{CaV}_4\text{O}_9$ .<sup>30</sup> This might be because of the formation of  $\text{V}^{4+}$ –O double bonds as in coordination compounds.<sup>31</sup> However, we propose another scenario based on our magnetic studies. The  $\text{V}^{4+}$  ion has a  $d^1$  electronic configuration, and an LDA calculation has shown that a single d electron of the  $\text{V}^{4+}$  ion in a pyramidal coordination generally occupies the nondegenerate  $d_{xy}$  orbital.<sup>32</sup> This can be intuitively understood as follows. If a Jahn–Teller (J–T) distortion takes place in such a way that the V–O bonds expand in the tetragonal  $c$  direction, the energy of the  $d_{xy}$  orbital should be higher than the energies of the degenerate  $d_{yz}$  and  $d_{zx}$

(23) Shannon, N.; Schmidt, B.; Penc, K.; Thalmeier, P. *Eur. Phys. J. B* **2004**, *38*, 599.

(24) Sushkov, O. P.; Oitmaa, J.; Zheng, W. H. *Phys. Rev. B* **2001**, *6310*, 104420.

(25) Siurakshina, L.; Ihle, D.; Hayn, R. *Phys. Rev. B* **2001**, *6410*, 104406.

(26) Matsuda, M.; Yamada, K.; Kakurai, K.; Kadowaki, H.; Thurston, T. R.; Endoh, Y.; Hidaka, Y.; Birgeneau, R. J.; Kastner, M. A.; Gehring, P. M.; Moudden, A. H.; Shirane, G. *Phys. Rev. B* **1990**, *42*, 10098.

(27) Vaknin, D.; Caignol, E.; Davies, P. K.; Fischer, J. E.; Johnston, D. C.; Goshorn, D. P. *Phys. Rev. B* **1989**, *39*, 9122.

(28) Hiroi, Z.; Azuma, M.; Fujishiro, Y.; Saito, T.; Takano, M.; Izumi, F.; Kamiyama, T.; Ikeda, T. *J. Solid State Chem.* **1999**, *146*, 369.

(29) Azuma, M.; Saito, T.; Fujishiro, Y.; Hiroi, Z.; Takano, M.; Izumi, F.; Kamiyama, T.; Ikeda, T.; Narumi, Y.; Kindo, K. *Phys. Rev. B* **1999**, *60*, 10145.

(30) Bouloux, J. C.; Galy, J. *Acta Crystallogr., Sect. B* **1973**, *B 29*, 1335.

(31) Butler, A.; Clague, M. J.; Meister, G. E. *Chem. Rev.* **1994**, *94*, 625–638.

(32) Korotin, M. A.; Elfimov, I. S.; Anisimov, V. I.; Troyer, M.; Khomskii, D. I. *Phys. Rev. Lett.* **1999**, *83*, 1387.

(21) Keren, A.; Le, L. P.; Luke, G. M.; Sternlieb, B. J.; Wu, W. D.; Uemura, Y. J.; Tajima, S.; Uchida, S. *Phys. Rev. B* **1993**, *48*, 12926.

(22) Dawson, W. K.; Tibbs, K.; Weathersby, S. P.; Boekema, C.; Chan, K. C. B. *J. Appl. Phys.* **1988**, *64*, 5809.

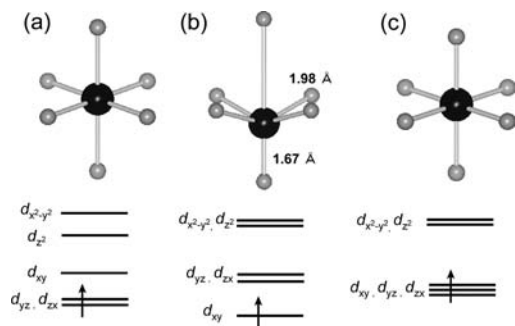


**Figure 4.** Schematic drawings of the  $\text{VO}_6$  octahedra with various distortions and the corresponding energy level diagrams for (a) Jahn–Teller distortion, (b) pyramidal coordination, and (c) no distortion.

orbitals (Figure 4a). In this case, the orbital degeneracy remains. Another fashion of J–T distortion where the octahedron shrinks in the  $c$  direction as found in the  $\text{V}^{3+}$  systems<sup>33</sup> is not favored in this system because of the stereochemical effect of the  $\text{Pb}^{2+}$  ions. In the local V–O configuration in the noncentrosymmetric  $\text{VO}_6$  octahedron of this system, which can be regarded as rather pyramidal, one of the V– $\text{O}_{\text{apex}}$  bonds is significantly shorter than the V– $\text{O}_{\text{in-plane}}$  bonds (Figure 4b). The d electron tends to avoid this close  $\text{O}_{\text{apex}}$ , so the energy of  $d_{xy}$  orbital is lowered. In other words, pyramidal coordination is stabilized in the  $d^1$  system to lift the orbital degeneracy. The  $6s^2$  lone pairs of  $\text{Pb}^{2+}$  are therefore aligned along the  $c$  direction and further enhance the distortion. This is the origin of the large tetragonal distortion and the two-dimensional magnetism in  $\text{PbVO}_3$ . This scenario explains the pressure-induced metallization of  $\text{PbVO}_3$  we reported previously.<sup>8</sup> The insulating nature of  $\text{PbVO}_3$  is due to the ordering of the  $d_{xy}$  orbital as discussed before.<sup>34</sup> If cubic  $\text{PbVO}_3$  is obtained, the three  $t_{2g}$  orbitals will be degenerate (Figure 4c), so metallic conductivity is

expected as in the cubic  $\text{SrVO}_3$ . Indeed, a pressure induced tetragonal to cubic transition associated with an insulator to metal transition was observed at 3 GPa.<sup>8</sup> This supports our speculation that the  $d^1$  electronic configuration plays a role in the large tetragonal distortion.

Accordingly, a similar large  $\text{PbTiO}_3$ -type distortion in  $\text{BiCoO}_3$  can also be explained. The  $\text{Co}^{3+}$  ion has a  $d^6$  electronic configuration. If five electrons are distributed to each of the five d orbitals, tetragonal distortion is induced so that the last one goes into the nondegenerate  $d_{xy}$  orbital as in the  $d^1$  system. This scenario is consistent with the experimentally confirmed high-spin  $t_{2g}^4 e_g^2$  state of  $\text{Co}^{3+}$  in  $\text{BiCoO}_3$ .<sup>10</sup> We predict that the  $d^1$  electronic configuration of  $\text{Ti}^{3+}$  will cause  $\text{BiTiO}_3$  stabilized in a perovskite structure to have a large tetragonal distortion like that of  $\text{PbVO}_3$ .

## 5. Conclusions

The magnetic properties of perovskite  $\text{PbVO}_3$  were investigated by means of magnetization measurements on pure single-crystalline samples and by  $\mu\text{SR}$  measurements. This compound was found to be a two-dimensional antiferromagnet with a long-range ordering temperature of 43–50 K. The two-dimensional magnetism is due to the ordering of  $d_{xy}$  orbitals, which is also considered to play an important role for the tetragonal distortion of  $\text{PbVO}_3$ .

**Acknowledgment.** The authors express their thanks to Prof. Tamio Oguchi for fruitful discussions. This work was supported by the MEXT of Japan Grants-in-Aid for Scientific Research (17105002, 18350097, 19GS0207, 19014010, 19340098, and 19052008) and for Joint Project of Chemical Synthesis Core Research Institutions and Elements Science and Technology Project. The synchrotron radiation experiments were performed at the SPring-8 with the approval of the Japan Synchrotron Radiation Research Institute.

IC800649A

(33) Suzuki, T.; Katsumura, M.; Taniguchi, K.; Arima, T.; Katsufuji, T. *Phys. Rev. Lett.* **2007**, *98*, 127203.

(34) Pickett, W. E. *Phys. Rev. Lett.* **1997**, *79*, 1746.